

REPORT DOCUMENTATION PAGE				Form Approved OMB NO. 0704-0188	
<p>The public reporting burden for this collection of information is estimated to average 1 hour per response, including the time for reviewing instructions, searching existing data sources, gathering and maintaining the data needed, and completing and reviewing the collection of information. Send comments regarding this burden estimate or any other aspect of this collection of information, including suggestions for reducing this burden, to Washington Headquarters Services, Directorate for Information Operations and Reports, 1215 Jefferson Davis Highway, Suite 1204, Arlington VA, 22202-4302. Respondents should be aware that notwithstanding any other provision of law, no person shall be subject to any penalty for failing to comply with a collection of information if it does not display a currently valid OMB control number.</p> <p>PLEASE DO NOT RETURN YOUR FORM TO THE ABOVE ADDRESS.</p>					
1. REPORT DATE (DD-MM-YYYY) 16-03-2009		2. REPORT TYPE New Reprint		3. DATES COVERED (From - To) 16-Mar-2009 -	
4. TITLE AND SUBTITLE Spatially resolved photocurrent mapping of operating organic photovoltaic devices using atomic force photovoltaic microscopy				5a. CONTRACT NUMBER W911NF-05-1-0177	
				5b. GRANT NUMBER	
				5c. PROGRAM ELEMENT NUMBER 611103	
6. AUTHORS B. J. Leever, M. F. Durstock, M. D. Irwin, A. W. Hains, T. J. Marks, L. S. C. Pingree, and M. C. Hersam				5d. PROJECT NUMBER	
				5e. TASK NUMBER	
				5f. WORK UNIT NUMBER	
7. PERFORMING ORGANIZATION NAMES AND ADDRESSES Northwestern University Office of Sponsored Research Northwestern University Evanston, IL 60208 -1110				8. PERFORMING ORGANIZATION REPORT NUMBER	
9. SPONSORING/MONITORING AGENCY NAME(S) AND ADDRESS(ES) U.S. Army Research Office P.O. Box 12211 Research Triangle Park, NC 27709-2211				10. SPONSOR/MONITOR'S ACRONYM(S) ARO	
				11. SPONSOR/MONITOR'S REPORT NUMBER(S) 48138-CH-PCS.5	
12. DISTRIBUTION AVAILABILITY STATEMENT Approved for public release; federal purpose rights					
13. SUPPLEMENTARY NOTES The views, opinions and/or findings contained in this report are those of the author(s) and should not be construed as an official Department of the Army position, policy or decision, unless so designated by other documentation.					
14. ABSTRACT A conductive atomic force microscopy (cAFM) technique, atomic force photovoltaic microscopy (AFPM), has been developed to characterize spatially localized inhomogeneities in organic photovoltaic (OPV) devices. In AFPM, a biased cAFM probe is raster scanned over an array of illuminated solar cells, simultaneously generating topographic and photocurrent maps. As proof of principle, AFPM is used to characterize OPVs, revealing substantial device to device and temporal variations in the short-circuit current. The flexibility of AFPM suggests					
15. SUBJECT TERMS					
16. SECURITY CLASSIFICATION OF:			17. LIMITATION OF ABSTRACT SAR	15. NUMBER OF PAGES	19a. NAME OF RESPONSIBLE PERSON Mark Hersam
a. REPORT U	b. ABSTRACT U	c. THIS PAGE U			19b. TELEPHONE NUMBER 847-491-2696

## **Report Title**

Spatially resolved photocurrent mapping of operating organic photovoltaic devices using atomic force photovoltaic microscopy

### **ABSTRACT**

A conductive atomic force microscopy (cAFM) technique, atomic force photovoltaic microscopy (AFPM), has been developed to characterize spatially localized inhomogeneities in organic photovoltaic (OPV) devices. In AFPM, a biased cAFM probe is raster scanned over an array of illuminated solar cells, simultaneously generating topographic and photocurrent maps. As proof of principle, AFPM is used to characterize OPVs, revealing substantial device to device and temporal variations in the short-circuit current. The flexibility of AFPM suggests applicability to nanoscale characterization of a wide range of optoelectronically active materials and devices.



---

**REPORT DOCUMENTATION PAGE (SF298)**  
**(Continuation Sheet)**

---

Continuation for Block 13

ARO Report Number    48138.5-CH-PCS  
Spatially resolved photocurrent mapping of oper    ...

Block 13: Supplementary Note

© 2008 American Institute of Physics. Published in Applied Physics Letters, Vol. 92,013302 (2008), (02). DoD Components reserve a royalty-free, nonexclusive and irrevocable right to reproduce, publish, or otherwise use the work for Federal purposes, and to authorize others to do so (DODGARS §32.36). The views, opinions and/or findings contained in this report are those of the author(s) and should not be construed as an official Department of the Army position, policy or decision, unless so designated by other documentation.

Approved for public release; federal purpose rights

# Spatially resolved photocurrent mapping of operating organic photovoltaic devices using atomic force photovoltaic microscopy

B. J. Leever and M. F. Durstock

*Materials and Manufacturing Directorate, Air Force Research Laboratory, Wright Patterson AFB, Ohio 45433, USA*

M. D. Irwin, A. W. Hains, and T. J. Marks<sup>a)</sup>

*Department of Chemistry, Northwestern University, Evanston, Illinois 60208-3113, USA*

L. S. C. Pingree and M. C. Hersam<sup>b)</sup>

*Department of Materials Science and Engineering, Northwestern University, Evanston, Illinois 60208-3108, USA*

(Received 4 October 2007; accepted 10 December 2007; published online 4 January 2008)

A conductive atomic force microscopy (cAFM) technique, atomic force photovoltaic microscopy (AFPM), has been developed to characterize spatially localized inhomogeneities in organic photovoltaic (OPV) devices. In AFPM, a biased cAFM probe is raster scanned over an array of illuminated solar cells, simultaneously generating topographic and photocurrent maps. As proof of principle, AFPM is used to characterize  $7.5 \times 7.5 \mu\text{m}^2$  poly(3-hexylthiophene):[6,6]-phenyl-C<sub>61</sub>-butyric acid methyl ester OPVs, revealing substantial device to device and temporal variations in the short-circuit current. The flexibility of AFPM suggests applicability to nanoscale characterization of a wide range of optoelectronically active materials and devices. © 2008 American Institute of Physics. [DOI: 10.1063/1.2830695]

The performance of organic photovoltaic (OPV) devices is most frequently characterized by the power conversion efficiency  $\eta_p$ , which indicates the percentage of the radiant energy incident on the solar cell that is converted to electrical energy, and is determined by measuring the open-circuit voltage ( $V_{oc}$ ), short-circuit current ( $I_{sc}$ ), and fill factor from current-voltage plots.<sup>1,2</sup> Although  $\eta_p$  serves as a convenient benchmark for comparing photovoltaic devices, it does not reveal information about local photocurrent spatial variations within these devices. Localized efficiency variations might be expected in bulk-heterojunction (BHJ) OPVs from defects as well as from the interpenetrating phase-separated nature of the microstructure, evident in morphological studies by atomic force microscopy,<sup>3,4</sup> transmission electron microscopy,<sup>5</sup> scanning electron microscopy,<sup>6</sup> and scanning transmission x-ray microscopy.<sup>7</sup>

The correlations between electrical properties and morphology in bulk heterojunction OPV films have previously been demonstrated with scanning probe techniques. For example, a morphology-work function relationship in poly(2-methoxy-5-(3',7'-dimethyloctyloxy))-p-phenylene vinylene:[6,6]-phenyl-C<sub>61</sub>-butyric acid methyl ester (MDMO-PPV:PCBM) films was demonstrated by Kelvin probe force microscopy.<sup>8</sup> Similarly, a correspondence between morphology and photocurrent was established in polyfluorene films by near-field scanning photocurrent microscopy (NSPM).<sup>9</sup> While NSPM lateral resolution is limited to  $\sim 200$  nm by the tip aperture, conductive atomic force microscopy (cAFM) offers the potential to resolve current variations an order of magnitude smaller.<sup>10,11</sup> Previously, cAFM was used for current mapping in polymer/small molecule blends,<sup>12</sup> polymer/polymer blends,<sup>13</sup> and CdTe/CdS composite materials.<sup>14</sup>

Recently, two scanning probe techniques having sub-100-nm lateral spatial resolution and calibrated light sources were reported: (1) time-resolved electrostatic force microscopy was used to simultaneously measure localized photoinduced charging rates and topography in a polyfluorene film,<sup>15</sup> and (2) photoconductive AFM employed a laser to illuminate a BHJ film while measuring topography and photocurrent with a conductive platinum-coated probe.<sup>16</sup> While both techniques provide quantitative correlations between electrical properties and morphology, they characterize photovoltaic films rather than functioning photovoltaic devices. Herein, we present an alternative cAFM technique, atomic force photovoltaic microscopy (AFPM), which quantitatively characterizes variations in fully operational photovoltaic devices by scanning across an array of solar cells that include the metal cathodes. Analyzing devices more closely reproduces real-world operating conditions, enables standard photovoltaic figures of merit to be extracted, and minimizes substrate-cAFM tip contact effects.

Figure 1 shows a diagram and photograph of the AFPM experimental apparatus. As in our previously reported atomic force electroluminescence technique,<sup>17,18</sup> the glass substrate with the photovoltaic devices is attached to a lightweight ( $<5$  g) optics stage. The small stage mass minimizes interference with the piezoelectric scanner on which it rests. All experiments were performed in contact mode and ambient conditions on a ThermoMicroscopes CP Research AFM with Nanosensors boron-doped, diamond-coated silicon AFM probes (model DT-NCHR). The electrical connection is made to the indium tin oxide (ITO) anode by affixing a copper wire, and a DL Instruments current preamplifier measures the current through the cAFM probe, which scans across the array of cathodes at an applied force of 20–50 nN.

The devices are illuminated by a Newport Oriel 96000 solar light simulator. From the lamp housing, the light passes through an AM1.5G filter and then through a liquid light

<sup>a)</sup>Electronic mail: t-marks@northwestern.edu.

<sup>b)</sup>Electronic mail: m-hersam@northwestern.edu.

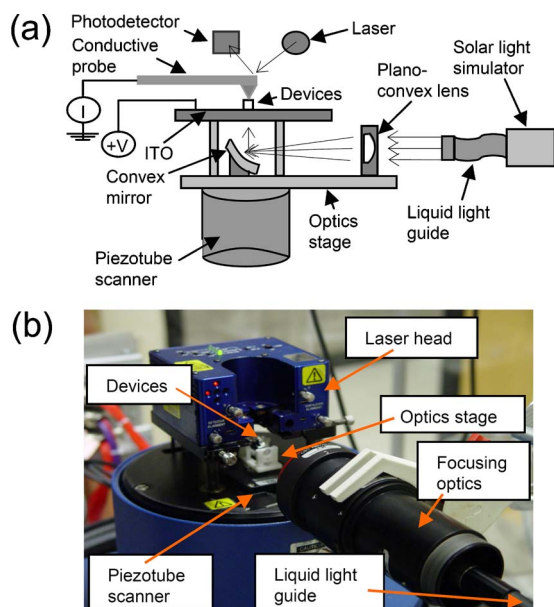


FIG. 1. (Color online) (a) Schematic diagram and (b) photograph of the AFPM experimental apparatus.

guide (Newport Oriel model 77638). Optics at the exit of the liquid light guide focus and collimate the light into a plano-convex lens on the optics stage. Finally, the light is focused by this lens onto a convex mirror and reflected onto the substrate, thereby illuminating the solar cells. The intensity of light reaching the substrate is measured by an Orion TH power meter and can be varied from  $\sim 6$  to 10 suns (1 sun =  $100 \text{ mW/cm}^2$ ). Although some light reaches the photodiode in the AFM feedback loop, simply nulling the cantilever deflection signal after illumination allows normal scanning.

ITO-coated glass (sheet resistance of  $\sim 10 \text{ } \Omega/\text{sq}$ , rms roughness of  $\sim 2.5 \text{ nm}$ ) purchased from Delta Technologies serves as the substrate for all devices. Before film deposition, the substrates are cleaned with a standard detergent/de-ionized water/solvent sonication process and then treated with UV ozone or an  $\text{O}_2$  plasma. Poly(3-hexylthiophene) (P3HT) was purchased from Rieke Metals and the PCBM from American Dye Source; both were purified by standard techniques.

In a glovebox ( $<1 \text{ ppm O}_2$ ), the cleaned ITO substrates are spin coated for 60 s at 550 rpm with a 1:1 solution of P3HT:PCBM dissolved in purified 1,2-dichlorobenzene.<sup>19</sup> The films are allowed to dry in the glovebox and then annealed at  $\sim 110^\circ\text{C}$ . Although such devices are often dried slowly in covered Petri dishes,<sup>19,20</sup> the shorter drying times used here

( $<5 \text{ min}$ ) reduced film roughness and significantly improved the probe-sample contact. Finally,  $7.5 \times 7.5 \text{ } \mu\text{m}^2$  gold cathodes are thermally evaporated through a copper mesh transmission electron microscope grid (Ted Pella, Inc.) at  $0.2\text{--}0.3 \text{ } \text{\AA}/\text{s}$  to a thickness of  $\sim 50 \text{ nm}$  on the P3HT:PCBM film. Gold is used as the cathode material because of its resistance to oxidation under the ambient test conditions.

Figure 2 shows simultaneous AFPM topography-current maps from P3HT:PCBM OPVs fabricated without a poly(3,4-ethylenedioxythiophene):poly(styrenesulfonate) PEDOT:PSS layer. The current maps in Figs. 2(b) and 2(c) were collected sequentially from the same set scan area, with the sample bias changed from  $0.0 \text{ V}$  ( $I_{\text{sc}}$ ) in the former to  $-0.50 \text{ V}$  in the latter. The devices were illuminated at  $\sim 6.7$  suns in both scans. The scans show similar device-to-device variations, including a difference in  $I_{\text{sc}}$  of up to  $\sim 25\%$  between OPVs separated by  $<10 \text{ } \mu\text{m}$ . As phase separation is known to occur in these films at length scales far smaller than the  $56 \text{ } \mu\text{m}^2$  area of these devices,<sup>5,21</sup> the observed current variations are likely due to inhomogeneities or defects occurring at larger length scales in the solar cells.

Variations in the electrical conductivity of the ITO surface, for example, have been observed by cAFM and attributed to the nonstoichiometric nature of the ITO as well as to organic contaminants.<sup>22,23</sup> Similar variations are observed in organic light-emitting diodes (OLEDs) of the same scale due to a variable charge trap density at the ITO/hole transport layer interface.<sup>18</sup> Furthermore, pinholes in the cathode and corrosion at the cathode/organic interface have been shown to cause dark spots in OLEDs (Ref. 24 and 25) and could be expected to analogously reduce the current density of OPV devices. Solar cells with a PEDOT:PSS layer also exhibit variation similar to that in Fig. 2, which could be influenced by regions of enhanced conductivity that have been reported to be up to several hundred nanometers in spatial extent.<sup>26</sup> Finally, photocurrent uniformity could be influenced by variations in the bulk P3HT:PCBM film.

In addition to scanning device arrays, solar cells can also be individually addressed by the cAFM probe to measure current-voltage characteristics. These devices exhibit S-shaped  $I$ - $V$  plots and low fill factors ( $\sim 18.5\%$ ), characteristic of marginal active layer/cathode interfaces.<sup>27</sup> This behavior is not surprising considering that LiF was not applied prior to gold deposition and because the deposition conditions are significantly harsher for gold than for aluminum. The devices exhibit a short-circuit current density of  $\sim 18 \text{ mA/cm}^2$  (under 6.7 suns illumination), an open-circuit

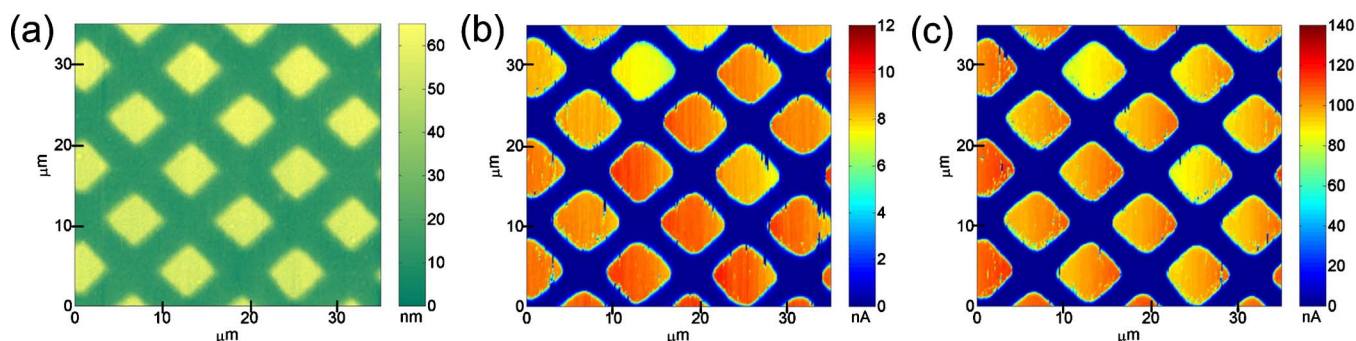


FIG. 2. (Color online) (a) AFPM topographic map of a  $7.5 \times 7.5 \text{ } \mu\text{m}^2$  OPV array. (b) AFPM current map at  $0.0 \text{ V}$  applied bias and (c) AFPM current map at  $-0.50 \text{ V}$  applied bias. In the AFPM current maps, the absolute value of the photocurrent is depicted.



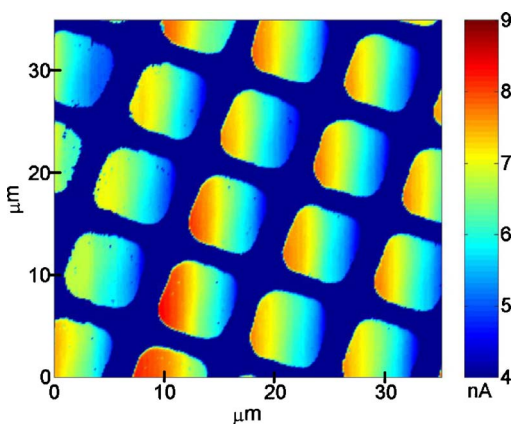


FIG. 3. (Color online) Short-circuit transient response of OPV devices in air. Devices are illuminated at 6.7 suns and are initially contacted at the left edge. Note that the absolute value of the photocurrent is depicted and that the current scale bar is truncated compared to Fig. 2.

voltage of  $\sim 225$  mV, and a power conversion efficiency of  $\sim 0.11\%$ .

Scanning the OPVs at a constant bias also reveals temporal variations in the photocurrent under ambient conditions. Although these temporal variations are present in Fig. 2, they are more easily visualized when the current scale of the photocurrent map is truncated, as in Fig. 3. In Fig. 3, devices scanned at  $I_{sc}$  exhibit a transient response with  $I_{sc}$  decaying by  $\sim 40\%$  during the  $\sim 1$  min that the probe is in contact with the device (fast scan direction is top to bottom; slow scan direction is left to right). Different substrates scanned at different tip speeds show essentially the same decay rate, which exceeds the reported degradation rate for similar devices due to air and light exposure.<sup>28</sup> The increased degradation rate is likely related to factors including the high illumination intensity, the large portion of the active layer exposed directly to air, the thinness of the cathode, and the nonoptimum active layer/cathode interface.<sup>29</sup>

In summary, AFPM has been demonstrated as a technique to quantitatively measure spatial performance variations in functioning OPVs. Microscopic solar cells can be individually addressed, enabling quantification of local  $\eta_p$  and other benchmarks. Furthermore, temporal variations in OPV response can be directly visualized. The flexibility of AFPM suggests its use in a variety of future studies. Possibilities include evaluating defect density and  $\eta_p$  as a function of device area, as well as increasing spatial resolution through the use of smaller electrodes. Other options include fabricating devices with alternative transparent electrodes and/or different photoactive layers to elucidate performance-spatial inhomogeneity relationships in photovoltaic cells.

This research was supported by BP Solar, DOE (DE-FG02-06ER46320), NSF (ECS-0609064), and AFRL Materials & Manufacturing Directorate. We also acknowledge the

use of facilities supported by the Northwestern University MRSEC (NSF DMR-0520513) and thank N. Cortes and M. Russell for many helpful suggestions and comments.

- <sup>1</sup>P. Peumans, A. Yakimov, and S. R. Forrest, *J. Appl. Phys.* **93**, 3693 (2003).
- <sup>2</sup>S. Gunes, H. Neugebauer, and N. S. Sariciftci, *Chem. Rev. (Washington, D.C.)* **107**, 1324 (2007).
- <sup>3</sup>A. P. Smith, R. R. Smith, B. E. Taylor, and M. F. Durstock, *Chem. Mater.* **16**, 4687 (2004).
- <sup>4</sup>H. J. Snaith, A. C. Arias, A. C. Morteau, C. Silva, and R. H. Friend, *Nano Lett.* **2**, 1353 (2002).
- <sup>5</sup>X. Yang, J. Loos, S. Veenstra, W. J. H. Verhees, M. M. Wienk, J. M. Kroon, M. A. J. Michels, and R. A. J. Janssen, *Nano Lett.* **5**, 579 (2005).
- <sup>6</sup>H. Hoppe, M. Niggemann, C. Winder, J. Kraut, R. Hiesgen, A. Hinsch, D. Meissner, and N. S. Sariciftci, *Adv. Funct. Mater.* **14**, 1005 (2004).
- <sup>7</sup>C. R. McNeill, B. Watts, L. Thomsen, W. J. Belcher, N. C. Greenham, and P. C. Dastoor, *Nano Lett.* **6**, 1202 (2006).
- <sup>8</sup>T. Glatzel, H. Hoppe, N. S. Sariciftci, M. Ch. Lux-Steiner, and M. Komiyama, *Jpn. J. Appl. Phys., Part 1* **44**, 5370 (2005).
- <sup>9</sup>C. R. McNeill, H. Frohne, J. L. Holdsworth, and P. C. Dastoor, *Nano Lett.* **4**, 2503 (2004).
- <sup>10</sup>M. C. Hersam, A. C. F. Hoole, S. J. O'Shea, and M. E. Welland, *Appl. Phys. Lett.* **72**, 915 (1998).
- <sup>11</sup>H.-N. Lin, H.-L. Lin, S.-S. Wang, L.-S. Yu, G.-Y. Perng, S.-A. Chen, and S.-H. Chen, *Appl. Phys. Lett.* **81**, 2572 (2002).
- <sup>12</sup>O. Douhéret, L. Lutsen, A. Swinnen, M. Bresselge, K. Vandewal, L. Goris, and J. Manca, *Appl. Phys. Lett.* **89**, 032107 (2006).
- <sup>13</sup>A. Alexeev, J. Loos, and M. M. Koetse, *Ultramicroscopy* **106**, 191 (2006).
- <sup>14</sup>H. R. Moutinho, R. G. Dhere, C. S. Jiang, M. M. Al-Jassim, and L. L. Kazmerski, *Thin Solid Films* **514**, 150 (2006).
- <sup>15</sup>D. C. Coffey and D. S. Ginger, *Nat. Mater.* **5**, 735 (2006).
- <sup>16</sup>D. C. Coffey, O. G. Reid, D. B. Rodovsky, G. P. Bartholomew, and D. S. Ginger, *Nano Lett.* **7**, 738 (2007).
- <sup>17</sup>L. S. C. Pingree, M. M. Kern, B. J. Scott, T. J. Marks, and M. C. Hersam, *Appl. Phys. Lett.* **85**, 344 (2004).
- <sup>18</sup>L. S. C. Pingree, M. T. Russell, B. J. Scott, T. J. Marks, and M. C. Hersam, *Org. Electron.* **8**, 465 (2007).
- <sup>19</sup>G. Li, V. Shrotriya, J. Huang, Y. Yao, T. Moriarty, K. Emery, and Y. Yang, *Nat. Mater.* **4**, 864 (2005).
- <sup>20</sup>V. D. Mihailescu, H. Xie, B. de Boer, L. M. Popescu, J. C. Hummelen, P. W. M. Blom, and L. J. A. Koster, *Appl. Phys. Lett.* **89**, 012107 (2006).
- <sup>21</sup>W. Ma, C. Yang, X. Gong, K. Lee, and A. J. Heeger, *Adv. Funct. Mater.* **15**, 1617 (2005).
- <sup>22</sup>Y.-H. Liao, N. F. Scherer, and K. Rhodes, *J. Phys. Chem. B* **105**, 3282 (2001).
- <sup>23</sup>H.-N. Lin, S.-Y. Chen, G.-Y. Perng, and S.-A. Chen, *J. Appl. Phys.* **89**, 3976 (2001).
- <sup>24</sup>J. McElvain, H. Antoniadis, M. R. Hueschen, J. N. Miller, D. M. Roitman, J. R. Sheats, and R. L. Moon, *J. Appl. Phys.* **80**, 6002 (1996).
- <sup>25</sup>H. Aziz, Z. Popovic, C. P. Tripp, N.-X. Hu, A.-M. Hor, and G. Xu, *Appl. Phys. Lett.* **72**, 2642 (1998).
- <sup>26</sup>M. Kemerink, S. Timpanaro, M. M. De Kok, E. A. Meulenkaamp, and F. J. Touwslager, *J. Phys. Chem. B* **108**, 18820 (2004).
- <sup>27</sup>M. Glatthaar, M. Riede, N. Keegan, K. Sylvester-Hvid, B. Zimmermann, M. Niggemann, A. Hinsch, and A. Gombert, *Sol. Energy Mater. Sol. Cells* **91**, 390 (2007).
- <sup>28</sup>K. Kawano, R. Pacios, D. Poplavskyy, J. Nelson, D. D. C. Bradley, and J. R. Durrant, *Sol. Energy Mater. Sol. Cells* **90**, 3520 (2006).
- <sup>29</sup>Rashmi, A. K. Kapoor, U. Kumar, V. R. Balakrishnan, and P. K. Basu, *Pramana, J. Phys.* **68**, 489 (2007).